**Table 11.2** Selected list of probe sets induced by estragole.

| | |
|---|---|
| PPAR alpha pathway by IPA | |
| Acaa1a | 1456011_x_at |
| Acot1 /// Acot2 /// LOC100044830 | 1422997_s_at |
| Acot1 /// LOC100044830 | 1449065_at |
| Acot3 | 1422925_s_at |
| Acot4 | 1422076_at, 1422077_at |
| Acox1 | 1444518_at |
| Acsl1 | 1460316_at |
| Acsl5 | 1428082_at |
| Agpat6 | 1422841_at, 1450776_at |
| Crat | 1417008_at |
| Ehhadh | 1448382_at |
| Pdk4 | 1417273_at |
| Pex1 | 1428716_at |
| Pex11a | 1419365_at, 1449442_at |
| Pxmp4 | 1455438_at |
| P450s | |
| Cyp4a10 /// Cyp4a31 | 1424853_s_at |
| Cyp4a14 | 1423257_at |
| Cyp4a31 | 1440134_at |
| Transporters | |
| Slc12a7 | 1418257_at |
| Slc14a2 | 1426109_a_at |
| Slc16a1 | 1415802_at |
| Slc16a5 | 1434473_at |
| Slc22a5 | 1421848_at |
| Slc22a5 | 1450395_at |
| Slc23a2 | 1417329_at |
| Slc23a2 | 1417330_at |
| Slc25a20 | 1423108_at |
| Slc25a20 | 1423109_s_at |
| Slc25a42 | 1424790_at |
| Slc27a1 | 1422811_at |
| Slc29a3 | 1455731_at |
| Oxidative stress, apoptosis and cell proliferation | |
| Aifm2 | 1431143_x_at |
| Bcl2l13 | 1429539_at |
| Casp8 | 1424552_at |
| Cntrob | 1433958_at |
| Glrx | 1416592_at |
| Txnip | 1415996_at |
| Others | |
| Dnaic1 | 1437093_at, 1437094_x_at |
| Fabp2 | 1418438_at |
| Gyk | 1422703_at, 1422704_at |
| Klf10 | 1416029_at |
| Klf11 | 1437241_at |
| Oplah | 1424359_at |
| Paqr7 | 1435312_at, 1460674_at |

proliferation. Agonists of this receptor are carcinogenic towards rodent liver *via* mechanisms related to peroxisome proliferation.[6] At the same time, since peroxisome proliferation leads to lowering of serum triglyceride levels, PPAR-alpha is a molecular target for hypolipidemic drugs, such as clofibrate.

Here, we found that estragole induces a considerable number of genes known to be regulated by PPAR-alpha. The Percellome Explorer (PE) program, which automatically compares probe set lists, has identified clofibrate (81 probe sets), followed by di(2-ethylhexyl) phthalate (DEHP) (126 probe sets) as the two chemicals causing changes most similar to those evoked by estragole upon testing with the same experimental protocol (Figure 11.4) (the absolute numbers of common probe sets were normalized to the product of the numbers of altered probe sets in each study). The PE program also compares probe sets on the basis of time, in the present case 2 hours after administration. Such early-responding genes are considered to be direct or almost direct targets of a receptor(s) that is activated by the test chemicals. Again, the similarity of its pattern to those of clofibrate and DEHP[7,8] confirms that one of the primary receptors that binds estragole is the PPAR-alpha. Isozyme 4 of pyruvate dehydrogenase kinase (Pdk4), shown in Figure 11.4, has already been reported to be regulated by this latter compound. Ingenuity pathway analysis was then applied for comparison with reported information (Figure 11.5). Two hours after administration, TXNIP, Klf10, and KLF11 did not appear to be directly regulated by PPAR-alpha, even though these three genes have recently been reported to be under the regulation of this receptor,[9,10] albeit with no clear relationship to liver function. Dynein, axonemal, and intermediate chain 1 (Dnaic1) is induced 8 and 24 hours after administration of estragole and clofibrate, respectively, as well as by DEHP and its metabolite mono(2-ethylhexyl) phthalate (MEHP) at later time-points (Figure 11.6). Dnaic1 appears to play an important role in peroxisome biogenesis.[11,12] This delayed induction, compared to that of early-response genes such as Pdk4, might indicate that several mediators are located between PPAR-alpha and this gene. The nature of the pathway, together with a literature search, indicate that HNF4A and PEX13[13] may be involved, since the latter is induced slightly by estragole (not significantly) and clearly by clofibrate, DEHP, and MEHP (Figure 11.6).

Among the many isozymes of cytochrome P-450, Cyp4a10, Cyp4a14, and Cyp4a31 are induced significantly by estragole, as well as by clofibrate and DEHP. On the other hand, Cyp1a2, which is induced slightly by phenobarbital, was not up-regulated by estragole. All three of these Cyp4a's are considered to be regulated by PPAR-alpha. Whereas DEHP also induces Cyp2b10 and Cyp51, estragole and clofibrate do not. Phenobarbital also induces Cyp2b10 and Cyp51, but not the Cyp4a's. Thus, the present Percellome analysis indicates (Figure 11.7) that DEHP activates at least two receptors, both PPAR-alpha and the constitutive androstane receptor (NR1I3 or CAR), which regulates Cyp2b[14] and probably Cyp51.[15,16] In contrast, estragole and clofibrate activate PPAR-alpha, but not CAR.

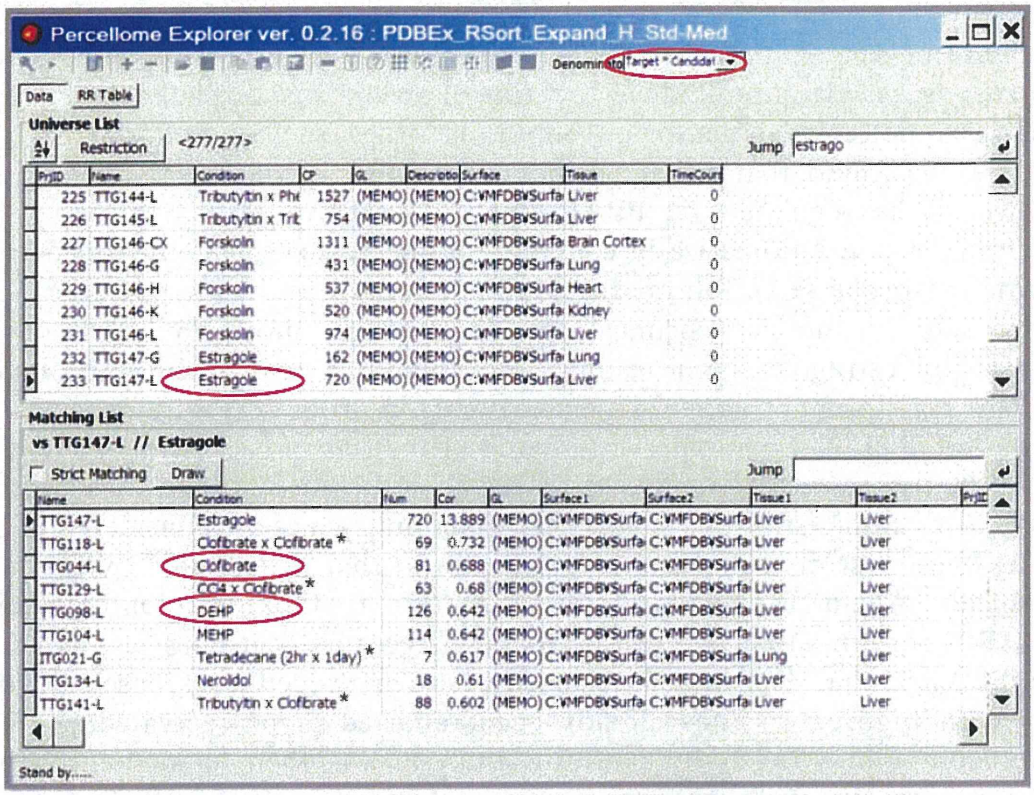


*:Performed by different protocols

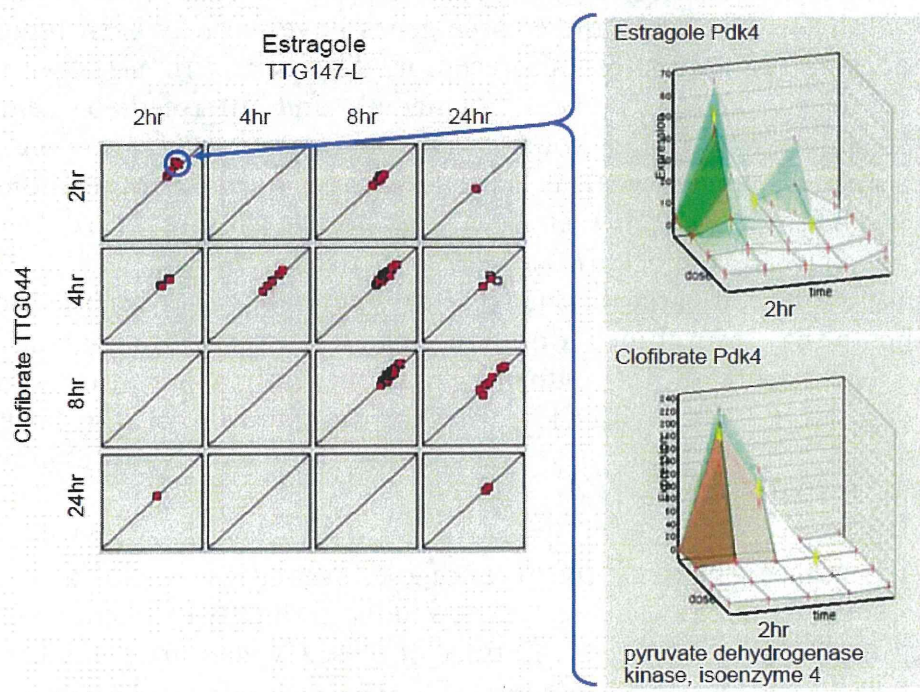


**Figure 11.4** Comparison of the similarity between various Percellome studies utilizing the Percellome Explorer program. The upper figure shows the calculations that identify clofibrate and DEHP as the top chemicals most similar to estragole. The lower figure illustrates the similar peak times of the probe sets common to estragole and clofibrate, using Pdk4 (1417273_at) as an example.

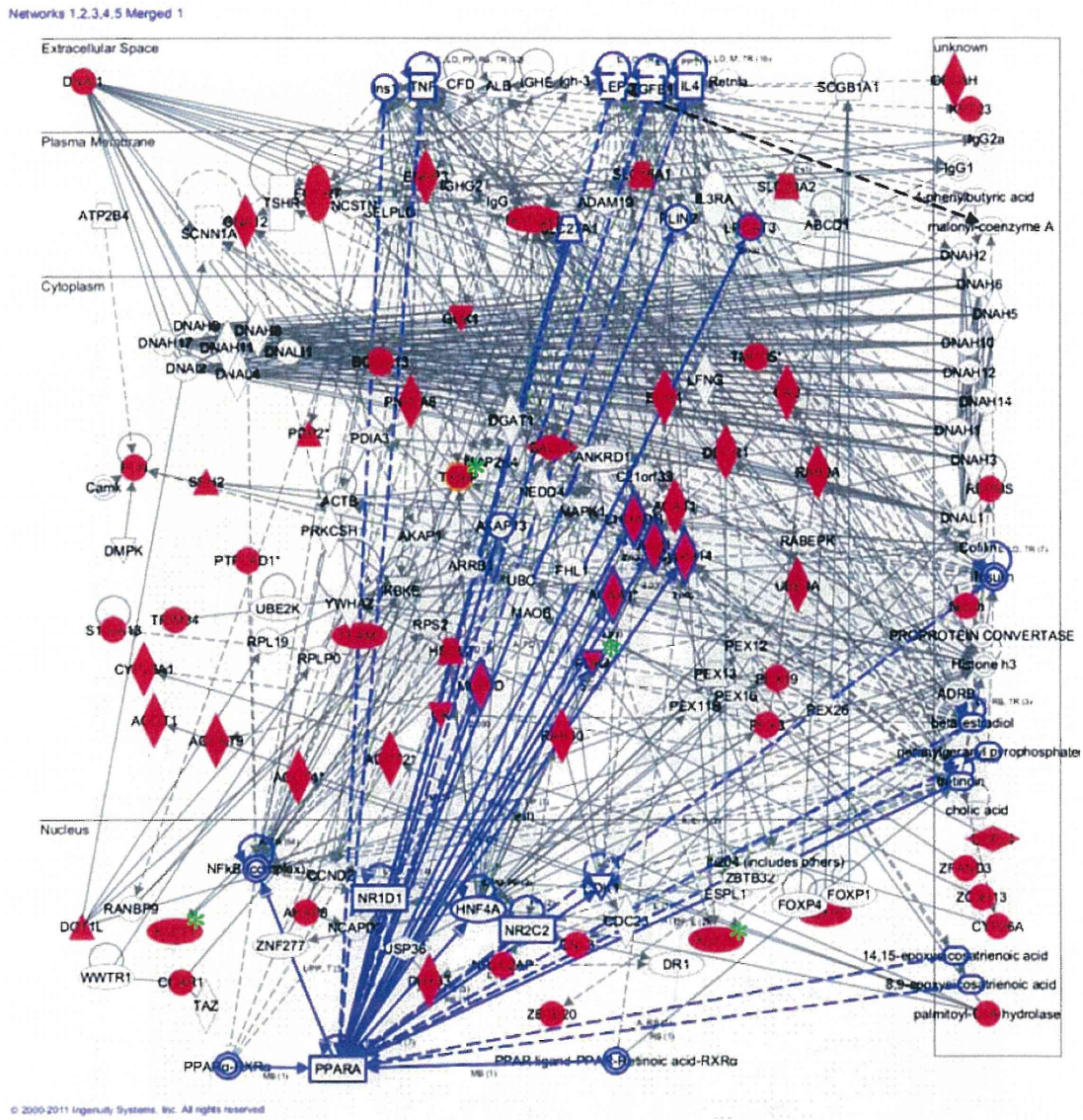


**Figure 11.5** Ingenuity pathway analysis of the probe sets common to estragole and clofibrate. Those elevated by both chemicals are highlighted in red. Among the four 2-h probe sets (green asterisk), only Pdk4 appears to be a direct target, whereas TXNIP, Klf10, and Klf11 appear to be influenced indirectly.

Expression of the drug and/or metal transporters Slc12a7, Slc14a2, Slc16a1, Slc16a5, Slc22a5, Slc23a2, Slc25a20, Slc25a42, Slc27a1, and Slc29a3 appeared here to be altered by estragole. Again, PE analysis reveals that most of these same Slc transporters are also induced by DEHP and clofibrate (not shown). Among these, only Slc27a1 has so far been reported to be regulated by PPAR-alpha.[17,18] However, expression of most of these Slc transporters, including Slc27a1, peaked after 8 hours, indicating that these genes may be activated indirectly.

Our novel finding that estragole activates PPAR-alpha signaling may help elucidate the mechanism(s) underlying estragole-induced carcinogenesis, *i.e.*

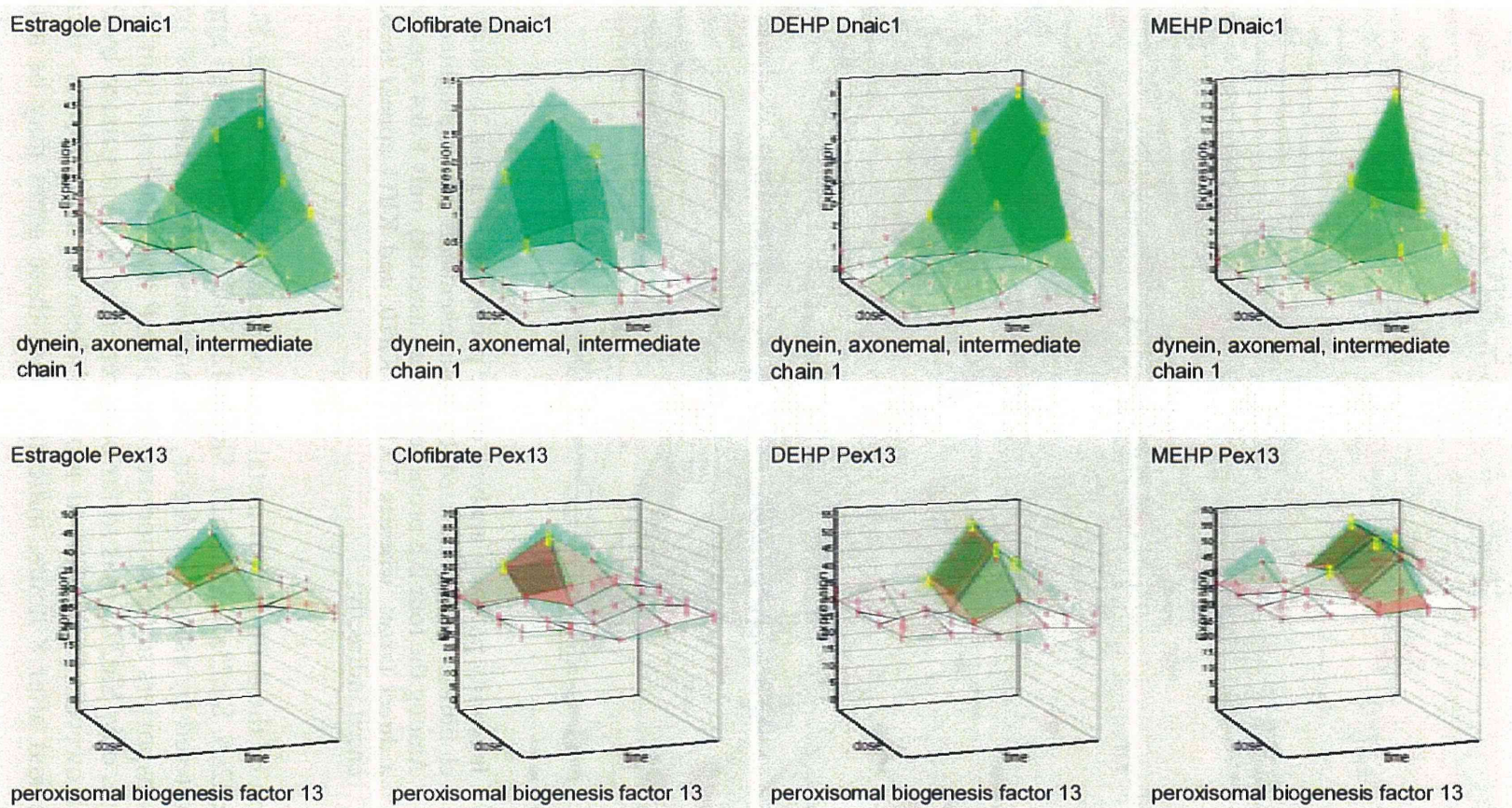


**Figure 11.6** The surface of Dnaic1 and Pex13 for estragole, clofibrate, DEHP, and MEHP. The late response may be mediated by Pex13.

peroxisome proliferation may be involved. Indeed, estragole increases liver weight at a dose lower than the carcinogenic dose.[19]

An important advantage in determining the actual average number of mRNA molecules per cell is that the responses obtained in different studies can be compared directly. As shown in Figures 11.6 and 11.7, the magnitude of the up-regulation of PPAR-alpha-inducible genes by estragole was comparable to that of clofibrate, since, at the same doses (*i.e.* 0, 10, 30, and 100 $mg \cdot kg^{-1}$) employed, estragole appears to be as potent as clofibrate in activating PPAR-alpha signaling.

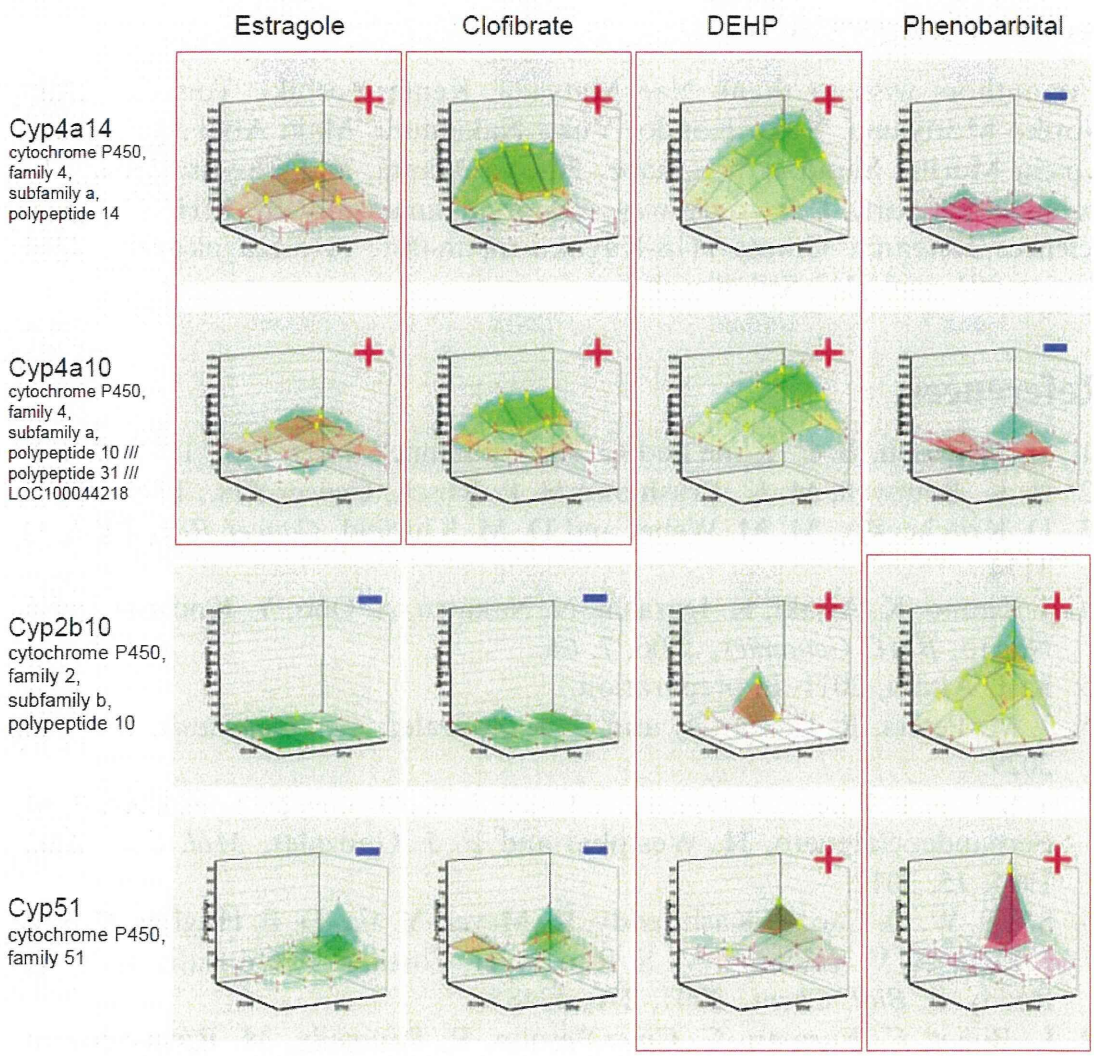


**Figure 11.7** Percellome analysis of representative P450s induced by estragole, clofibrate, DEHP, and phenobarbital. DEHP appears to induce P450s *via* at least two different pathways, *i.e.* PPAR-alpha and CAR, whereas estragole, clofibrate, and phenobarbital induce only PPAR-alpha or CAR, respectively.

## 11.5 Conclusions

Our present observations that estragole appears to be as potent an agonist of PPAR-alpha as clofibrate (on a $mg \cdot kg^{-1}$ basis) should now be confirmed by actual binding and signaling studies. If confirmed, the hepatocarcinogenic potential of this compound should be reevaluated accordingly. Although recent reports on estragole carcinogenicity suggest involvement of its metabolites[20] or glucocorticoid pathways,[21] our Percellome data support neither the involvement of such pathways or pronounced genotoxicity (which can be monitored indirectly as an enhancement in DNA repair and responses to oxidative stress). Interestingly, DEHP and Wyeth 14,643, well-characterized non-genotoxic rodent hepatocarcinogens that evoke tumors through peroxisome proliferation, gave mutation in Lac Z transgenic mice.[22]

## Acknowledgements

The authors wish to thank Nae Matsuda, Kenta Yoshiki, Tomoko Ando, Noriko Moriyama, Yuko Kondo, Yuko Nakamura, Maki Abe, Ayako Imai, Koichi Morita, Shinobu Watanabe, Hisako Aihara, and Chiyuri Aoyagi for technical support. This study was supported financially by MHLW Health Sciences Research Grants H18-Kagaku-Ippan-001, H15-Kagaku-002, H14-Toxico-001, and H13-Seikatsu-012.

## References

1. H. P. Rusch, B. E. Kline and C. A. Baumann, *Cancer Res.*, 1945, **5**, 431.
2. R. K. Boutwell, M. K. Brush and H. P. Rusch, *Cancer Res.*, 1949, **9**, 741.
3. D. Kritchevsky, M. M. Weber and D. M. Klurfeld, *Cancer Res.*, 1984, **44**, 3174.
4. J. Kanno, K. Aisaki, K. Igarashi, N. Nakatsu, A. Ono, Y. Kodama and T. Nagao, *BMC Genomics*, 2006, **7**, 64.
5. K.-I. Aisaki, 2011, in preparation.
6. J. M. Peters, R. C. Cattley and F. J. Gonzalez, *Carcinogenesis*, 1997, **18**, 2029.
7. S. S. Lee, T. Pineau, J. Drago, E. J. Lee, J. W. Owens, D. L. Kroetz, P. M. Fernandez-Salguero, H. Westphal and F. J. Gonzalez, *Mol. Cell. Biol.*, 1995, **15**, 3012.
8. S. Yu, W. Q. Cao, P. Kashireddy, K. Meyer, Y. Jia, D. E. Hughes, Y. Tan, J. Feng, A. V. Yeldandi, M. S. Rao, R. H. Costa, F. J. Gonzalez and J. K. Reddy, *J. Biol. Chem.*, 2001, **276**, 42485.
9. L. Billiet, C. Furman, C. Cuaz-Perolin, R. Paumelle, M. Raymondjean, T. Simmet and M. Rouis, *J. Mol. Biol.*, 2008, **384**, 564.
10. M. Rakhshandehroo, G. Hooiveld, M. Muller and S. Kersten, *PLoS One*, 2009, **4**, e6796.
11. C. B. Brocard, K. K. Boucher, C. Jedeszko, P. K. Kim and P. A. Walton, *Tra c*, 2005, **6**, 386.

12. C. Kural, H. Kim, S. Syed, G. Goshima, V. I. Gelfand and P. R. Selvin, *Science*, 2005, **308**, 1469.
13. D. T. Odom, N. Zizlsperger, D. B. Gordon, G. W. Bell, N. J. Rinaldi, H. L. Murray, T. L. Volkert, J. Schreiber, P. A. Rolfe, D. K. Gifford, E. Fraenkel, G. I. Bell and R. A. Young, *Science*, 2004, **303**, 1378.
14. H. Ren, L. M. Aleksunes, C. Wood, B. Vallanat, M. H. George, C. D. Klaassen and J. C. Corton, *Toxicol. Sci.*, **113**, 45.
15. J. G. Dekeyser, E. M. Laurenzana, E. C. Peterson, T. Chen and C. J. Omiecinski, *Toxicol. Sci.*, **120**, 381.
16. C. Xu, C. Y. Li and A. N. Kong, *Arch. Pharm. Res.*, 2005, **28**, 249.
17. G. A. Francis, E. Fayard, F. Picard and J. Auwerx, *Annu. Rev. Physiol.*, 2003, **65**, 261.
18. M. Lemoine, J. Capeau and L. Serfaty, *PPAR Res.*, 2009, **2009**, 906167.
19. FAO/WHO, 69th joint meeting, *Safety Evaluation of Certain Food Additives*, WHO Food Additives Series, International Programme on Chemical Safety, World Health Organization, Geneva, 2009.
20. Y. Ishii, Y. Suzuki, D. Hibi, M. Jin, K. Fukuhara, T. Umemura and A. Nishikawa, *Chem. Res. Toxicol.*, **24**, 532.
21. V. I. Kaledin, M. Y. Pakharukova, E. N. Pivovarova, K. Y. Kropachev, N. V. Baginskaya, E. D. Vasilieva, S. I. Ilnitskaya, E. V. Nikitenko, V. F. Kobzev and T. I. Merkulova, *Biochemistry (Moscow)*, 2009, **74**, 377.
22. M. E. Boerrigter, *J. Carcinog.*, 2004, **3**, 7.

Journal of Clinical and Experimental Medicine（IGAKU NO AYUMI）

[ISSN 0039-2359 CODEN:IGAYAY]

# 医学のあゆみ

第236巻・第12号（通巻2843）
2011年3月19日発行（毎週土曜日発行）
昭和21年7月27日第3種郵便物認可

Vol.236 No.12
2011
3/19

AYUMI

# 腎細胞癌の分子標的治療

腎細胞癌の分子標的治療の理論的根拠
分子標的治療の時代におけるサイトカイン治療の位置づけ
転移性腎細胞癌におけるsorafenib治療の意義
血管新生阻害薬：sunitinib――腎細胞癌治療における有効性と問題点
mTOR阻害剤：everolimus
転移性腎癌に対するmTOR阻害薬：temsirolimus
Pazopanib――腎癌治療における位置づけ
第二世代の血管新生阻害薬：axitinib

連載

**動物の感染症から学ぶ**
ヨーネ病――世界中に蔓延するウシの抗酸菌感染症

**逆システム学の窓**
あなたの職場の若者が結核排菌者と診断されたら
――患者へのサポートがDOTSを活かす

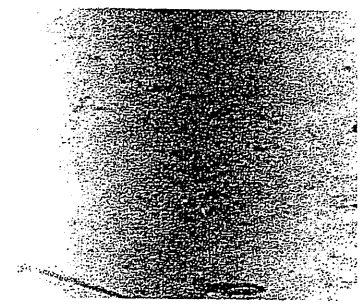

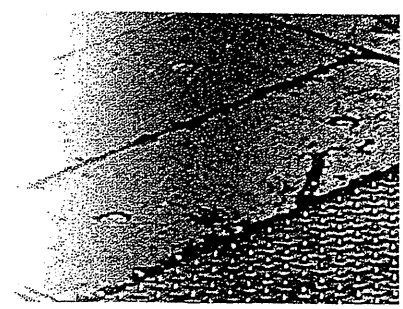

医歯薬出版株式会社
http://www.ishiyaku.co.jp/

医学のあゆみ Vol.236 No.12 2011/3/19

CONTENTS

AYUMI

# 腎細胞癌の分子標的治療

毒性学

# Percellomeトキシコゲノミクスの進捗

*Progress in percellome toxicogenomics*

## Percellomeトキシコゲノミクスプロジェクトとは

2006年に本誌の当欄にて，毒性学の高精度解析手法として開始した“Percellomeトキシコゲノミクスプロジェクト”を紹介させていただいた[1]．当毒性部の基本姿勢は変わらず，さまざまな物質が身体に取り込まれた際に生じる可能性のある毒性(有害性)を予測し，それらの使用に際しての被害を未然に防ぐのが毒性学の役割であるとの考えに立脚し，身のまわりにあり，体のなかに入ってくるすべての“もの”について，どのような場合に(胎児・新生児・小児など，吸い込む・飲み込むなど)，どのくらいの量で，どのような症状が現れるか(急性毒性，発癌を含む慢性毒性，遅発性毒性など)について研究を継続している．

具体的には実験動物の診断所見をヒトに外挿すべく実施しているが，従来法では種差や個体差は“安全係数”により量的な安全マージンをとることで勘案されてきた．しかし，サリドマイド奇形に代表されるように，これには科学的な限界があり，“毒性学の近代化”が必要である．医薬品の場合はヒトで治験を行える場合があるが，それも胎児や新生児には実施困難であり，一般的な物質の毒性を検討することを考えると現状では動物実験は不可避である．そこで，著者らはヒトの身代りとしての実験動物(遺伝子改変動物の活用を含む)を対象とした，Percellomeトキシコゲノミクス研究を開始した次第である．

これは生体というブラックボックスの中身を遺伝子発現ネットワークの面から解明することにより，生体反応メカニズムに基づいた分子毒性学を構築することを目的としている．その際，毒性を見落とさない“網羅性”を確保する必要性から，全遺伝子のトランスクリプトーム情報のなかから生物学的に有意と判断される反応ネットワークを網羅的に抽出するアプローチをとっている．複数の実験から得られる大量のデータを蓄積し横断的な解析を加えることが必須であることから，マイクロアレイデータの標準化と互換性確保のために“細胞1個当りのmRNAコピー数”を得るPercellome法[2]を開発し，プロジェクトを軌道に乗せたところまでを前回の記事でご紹介した．

## 最近の展開

その後の数年間に，100種類超(医薬品，一般化学物質，食品関連物質を含む)の化学物質によるマウス肝の初期応答データを含む，延べ3.5億遺伝子情報からなるPercellomeデータベースを得た．これは，基本的に投与後の時間，曝露用量，遺伝子発現量の3軸からなる三次元曲面データにより構成される(図1)．解析には，この三次元曲面の特徴抽出という独創的な方法をとり，解析ソフトウェア群(相崎健一ら)は独自開発である．また，動物実験レベルからのシステム管理により，高精細かつ高再現性を実現している．

得られたデータの例としては，アリル炭化水素受容体(AhR)に結合するダイオキシン(2, 3, 7, 8-TCDD)が比較的少数のAhR直下の遺伝子の発現を2時間目に誘導し，4, 8, 24と時間が経過する

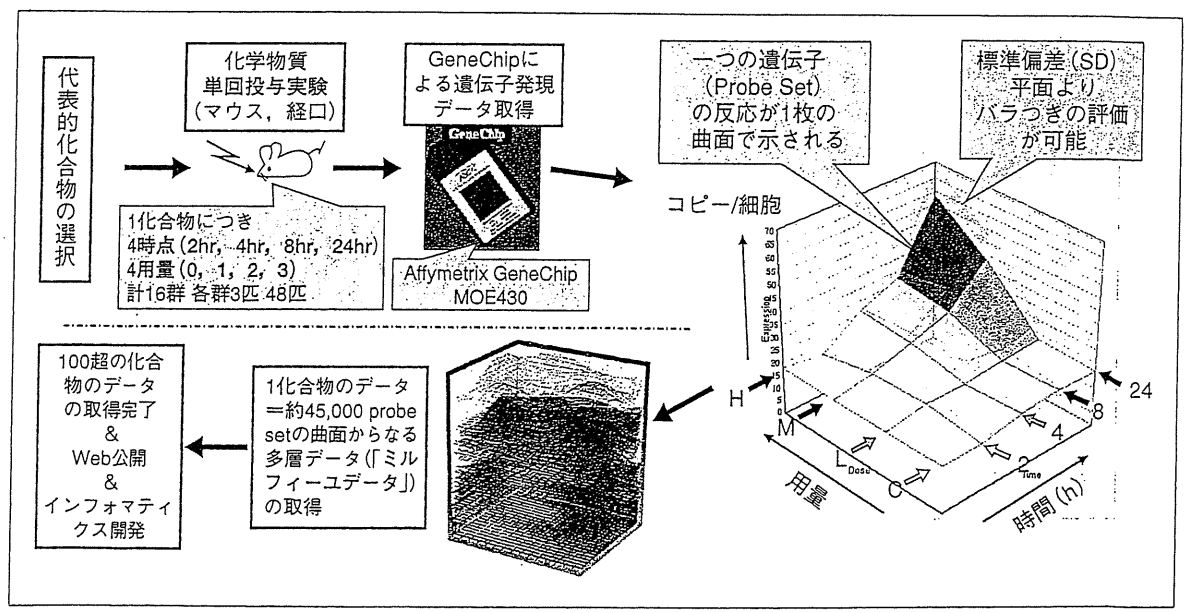


図1　Percellomeデータベースの概要

につれ数を増す状況が確認された．ダイオキシンの体内半減期が25時間であるにもかかわらず，2時間目のみの一過性発現のパターンをとるもの，持続的に発現が増加するものなどが観測されている．シックハウス症候群の指針値程度の，ごく低濃度域での吸入毒性トキシコゲノミクスも実施しており，ごく低濃度のホルマリン(0.1 ppm 付近)で肺の複数の遺伝子発現が明確に誘導されることをみている．サリドマイドは近年，癌治療薬として使用されていることから，複数の臓器における初期誘導を観測したところ，肺の2時間目に用量相関性をもって発現誘導のピークを示す遺伝子に，Cdkn1a (P21)が認められた．類似の発現パターンを示す初期応答遺伝子には，Fas，Foxo3a，Gata2など50あまりがあり，酸化的ストレスが誘発されることが推測された．実際，癌患者にサリドマイドが間質性肺炎を誘発する報告が増加しており，ヒトで確認された形となっている．

また，Percellome トキシコゲノミクスを発生毒性へも適用している．妊娠マウスにサリドマイドを投与し胎児で発現変動が認められた遺伝子のなかに，マウス胚の肢部形成に重要な分子が見出され(その遺伝子をノックアウトしたマウス胚にアザラシ肢症に類似の奇形が生じる)，サリドマイド奇形の標的分子検索の糸口が示唆された．さらに，胎生期～幼若期の発達中の脳に対する神経シグナル撹乱が脳構造や神経回路の形成に影響を及ぼし，成熟後に行動異常などの脳高次機能の障害として顕在化することを見出している．これについては，妊娠マウスへ神経伝達物質類似物質を投与し，生まれたマウスに誘発される遅発性中枢毒性と海馬の遺伝子発現異常の関連解析から標的ネットワークが示唆されつつある．

このほかにも投与した化学物質に関して，いままで報告のないあらたな遺伝子発現変動現象を多数見出し，そのいくつかには特定の毒性との連鎖を示唆する分子生物学的情報がみつかっていることから，それらを順次報告および一般公開する準備を進めている(http://www.nihs.go.jp/tox/TTG_Archive.htm；現在更新中．2010年度中再開予定)．

## プロジェクトの今後

さらに，マイクロアレイのクロスハイブリダイゼーションを修正するアルゴリズムの開発を終え(特許出願準備中)，その実装準備中である(NTT データおよび日本テラデータとの委託共同研究)．また，遺伝子ネットワークと毒性の動的な因果関係を導き出すインフォマティクスの構築研究やPercellome データの統合的提示方法の開発にも本格的に取り組んでおり(ソニーコンピュータサイエンス研究所との共同研究)，段階的に皆様にご披露できる予定である(厚生労働科学研究費補助金，環境研究総合推進費などによる)．


1) 菅野　純：毒性の高精細解析に向けてのトキシコゲノミクス．医学のあゆみ，218：1035-1036，2006.
2) Kanno, J. et al.："Per cell" normalization method for mRNA measurement by quantitative PCR and microarrays. *BMC Genomics*, 7：64, 2006.



菅野　純／Jun KANNO
国立医薬品食品衛生研究所
安全性生物試験研究センター毒性部


循環器内科学

# 心筋トロポニンの高感度測定の有用性

*Clinical utility of high-sensitivity cardiac troponin assay*

従来の心筋トロポニン測定は検出感度が低いため，急性冠症候群の診療以外で用いられることはまれであった．最近，検出感度が5倍以上改善された高感度測定が臨床の場に登場した．この高感度測定は，従来測定では検出不可能であった小さな心筋障害を診断できる．そのため，超急性期の心筋梗塞診断の精度[1,2]や慢性心不全における予後予測の精度[3]を高めることが示されている．さらに，外来診療や検診・人間ドック分野へのあらたな展開も期待される．

## 急性冠症候群の診療

トロポニンが上昇している不安定狭心症は，突然死や急性心筋梗塞発症の危険度が高い．このトロポニンの上昇は，破砕したプラークや血栓が引き起した末梢の微小塞栓による微小心筋障害を反映している．そのため，2000年に公表されたヨーロッパ心臓病学会/アメリカ心臓病学会(ESC/ACC)の心筋梗塞の再定義[4]は，トロポニンが上昇している不安定狭心症を急性心筋梗塞に包括した．さらに，ヨーロッパ心臓病学会/アメリカ心臓病学会/アメリカ心臓協会/世界心臓協会(ESC/ACC/AHA/WHF)の共同タスクフォースは，2007年に急性心筋梗塞の診断基準の再改定[5]を公表した．新しい診断基準では，トロポニンの心筋梗塞診断における基準値を健常人の99$^{th}$パーセンタイル値より大と定めた．一般に，測定値の相対的なばらつき(変動係数．coefficient of variation：CV)が小さいほど測定値の精度は高い．共同タスクフォースは試薬の精度にも言及しており，健常人の99$^{th}$パーセンタイル値における変動係数が10%以下である試薬を用いることを推奨した．従来の試薬はこの条件を

The Journal of Toxicological Sciences (J. Toxicol. Sci.)
Vol.37, No.2, 373-380, 2012



*Original Article*

# Development of humanized steroid and xenobiotic receptor mouse by homologous knock-in of the human steroid and xenobiotic receptor ligand binding domain sequence

**Katsuhide Igarashi[1], Satoshi Kitajima[1], Ken-ichi Aisaki[1], Kentaro Tanemura[1], Yuhji Taquahashi[1], Noriko Moriyama[1], Eriko Ikeno[1], Nae Matsuda[1], Yumiko Saga[2,3], Bruce Blumberg[4] and Jun Kanno[1]**

*[1]Division of Cellular and Molecular Toxicology, Biological Safety Research Center, National Institute of Health Sciences, 1-18-1 Kamiyoga, Setagaya-ku, Tokyo, 158-8501, Japan*
*[2]Division of Mammalian Development, National Institute of Genetics, Yata 1111, Mishima 411-8540, Japan*
*[3]The Graduate University for Advanced Studies (Sokendai), Yata 1111, Mishima 411-8540, Japan*
*[4]Department of Developmental and Cell Biology, 2011 Biological Sciences 3, University of California, Irvine, CA 92697-2300, USA*

(Received December 7, 2011; Accepted January 12, 2012)

**ABSTRACT** — The human steroid and xenobiotic receptor (SXR), (also known as pregnane X receptor PXR, and NR1I2) is a low affinity sensor that responds to a variety of endobiotic, nutritional and xenobiotic ligands. SXR activates transcription of Cytochrome P450, family 3, subfamily A (CYP3A) and other important metabolic enzymes to up-regulate catabolic pathways mediating xenobiotic elimination. One key feature that demarcates SXR from other nuclear receptors is that the human and rodent orthologues exhibit different ligand preference for a subset of toxicologically important chemicals. This difference leads to a profound problem for rodent studies to predict toxicity in humans. The objective of this study is to generate a new humanized mouse line, which responds systemically to human-specific ligands in order to better predict systemic toxicity in humans. For this purpose, the ligand binding domain (LBD) of the human SXR was homologously knocked-in to the murine gene replacing the endogenous LBD. The LBD-humanized chimeric gene was expressed in all ten organs examined, including liver, small intestine, stomach, kidney and lung in a pattern similar to the endogenous gene expressed in the wild-type (WT) mouse. Quantitative reverse transcription-polymerase chain reaction (RT-PCR) analysis showed that the human-selective ligand, rifampicin induced Cyp3a11 and Carboxylesterase 6 (Ces6) mRNA expression in liver and intestine, whereas the murine-selective ligand, pregnenolone-16-carbonitrile did not. This new humanized mouse line should provide a useful tool for assessing whole body toxicity, whether acute, chronic or developmental, induced by human selective ligands themselves and subsequently generated metabolites that can trigger further toxic responses mediated secondarily by other receptors distributed body-wide.

**Key words:** Steroid and xenobiotic receptor, Pregnane X receptor, Humanized mouse, Ligand binding domain, Knock-in mouse

## INTRODUCTION

Most orally administered xenobiotics are metabolized first by the intestine and then by the liver after portal transport. The expression levels of enzymes involved in xenobiotic metabolism are regulated at the transcriptional level by key xenobiotic sensors including the steroid and xenobiotic receptor (SXR), also known as the pregnane X receptor (PXR), pregnane activated receptor (PAR) and NR1I2 (Bertilsson *et al.*, 1998; Lehmann *et al.*, 1998; Blumberg *et al.*, 1998). SXR is important in the field of toxicology for at least two reasons. Firstly, this receptor system induces the expression of CYP3A and CYP2B enzymes, the major metabolizers of pharmaceu-

Correspondence: Jun Kanno (E-mail: kanno@nihs.go.jp)

ticals and xenobiotics. Therefore, SXR is a key mediator of drug- and chemical-induced toxicity as well as drug-drug and drug-nutrient interactions (Zhou *et al.*, 2004). Secondly, the orthologous rodent and human receptors exhibit differential sensitivity for a subset of chemical ligands important in the field of toxicology. For example, rifampicin (RIF) is a specific and selective activator of human SXR, whereas pregnenolone 16a-carbonitrile (PCN) is selective for the rodent orthologue.

Rodent-human differences in CYP3A and CYP2B-mediated responses to xenobiotics can be a profound problem in toxicologic studies where rodents are used to predict the toxicity of a compound in humans (Ma *et al.*, 2007). Therefore, development of a murine model that reconstructs the SXR-mediated systemic response of humans is of a great significance in toxicology.

Human and rodent SXRs share ~95% amino acid sequence identity in the DNA-binding domain (DBD) but only about 77% identity in the LBD. Tirona *et al.* (2004) analyzed the ligand selectivity of a human-rat chimeric protein and showed that the species differences are primarily defined by sequence differences in the LBD. Watkins and colleagues showed that the key residues responsible for the majority of the ligand selectivity were Leu 308 (human) and Phe305 (rat and mouse). Crystallographic analysis located these amino acids within or neighboring the flexible loop that forms a part of the pore to the ligand-binding cavity. Swapping the rodent and human-specific residues was shown to modulate the activation by the human-selective activator RIF *in vitro* (Watkins *et al.*, 2001). According to those findings, a simple replacement of the mouse LBD with the human sequence should be sufficient to "humanize" the ligand binding properties as well as activation of the downstream target genes.

Three kinds of humanized mice have already been generated. One is the SXR-null/Alb-SXR mouse (Alb-SXR mouse) made by crossing the SXR knockout mice with a transgenic mouse line that expresses human SXR in liver under the control of the albumin promoter (Xie *et al.*, 2000). Gonzalez and colleagues generated a transgenic mouse expressing a human BAC containing the entire hSXR gene in a SXR null background, thus controlled under human SXR promoter (SXR BAC mouse) (Ma *et al.*, 2007). Another mouse is the human SXR genome knock-in mice (hSXR genome mouse) (Scheer *et al.*, 2008). The human SXR genomic region from exon 2 to exon 9 was knocked-in to mouse SXR exon 2. This mouse expresses the human full length SXR mRNA under the control of mouse SXR promoter regulation. Although useful for toxicology studies, these mice have disadvantages in that the human SXR is expressed only in the liver (Alb-SXR mouse), hSXR mRNA is not expressed in all of the tissues where SXR is known to be expressed (SXR BAC mouse), and there might be potential differences in the binding affinities of hSXR DNA-binding domain (DBD) to *cis*-acting elements in mouse SXR target genes (hSXR genome mouse).

As noted above, it is known that the critical differences between human and rodent ligand-selectivity reside in the LBD. Therefore, when our project to generate a humanized SXR mouse was initiated, we reasoned that altering the LBD would be sufficient to generate a humanized ligand selectivity. We decided to retain the mouse DBD to avoid any potential differences between the binding affinities of the chimeric receptor for cis-acting elements in the mouse genome. To maintain the tissue-specific expression pattern of the endogenous gene, we inserted the human cDNA encoding the region carboxyl-terminal to the DBD into the mouse gene. This retains all of the 5' and 3' regulatory elements in the mouse gene, as well as introns 1 and 2, which contain important elements for regulating SXR expression (Jung *et al.*, 2006).

Here we report a new line of mouse (hSXRki mouse) in which a cDNA encoding the human LBD is homologously recombined into the mouse gene after exon 3. The tissue distribution of the resulting chimeric mouse DBD-human LBD mRNA is comparable to that of the WT mouse. The hSXRki mouse showed a fully humanized response to the human-selective activator RIF in that the Cyp3a11 mRNA was induced in liver and mucosa of small intestine in response to RIF, but not the rodent-selective compound PCN. This new mouse line should provide a useful tool for assessing the whole body toxicity induced by a human selective SXR ligand itself and its subsequently generated metabolite(s) that can trigger further toxic responses through other pathways body-wide.

## MATERIALS AND METHODS

### Generation of hSXRki knock-in mice

A DNA fragment of mouse SXR intron 2 to exon 3 was PCR amplified using mouse BAC DNA (BAC clone No. RP23-351P21) as a template. Primers used were BAC39486FW and mSXR462RV (for sequences of the primers see Table1). This fragment was connected to the LBD of human SXR cDNA from amino acid 105 through the carboxyl terminus amplified by the PCR primers: hSXR904FW and hSXR1887RVEcoRI (template; human SXR cDNA). The 3'UTR of bovine growth hormone (BGH) was added to 3' to the terminal codon. This concatenated fragment was introduced to a vector, which

**Table 1.** List of primer pairs

| Purpose | Primer name | Sequence (5' to 3') |
|---|---|---|
| Targeting vector construction | BAC39486FW | CCATGGGTACCACGAATAACAA |
| | mSXR462RV | CATGCCACTCTCCAGGCA |
| | hSXR904FW | AAGAAGGAGATGATCATGTCCG |
| | hSXR1887RVEcoRI | CCGAATTCTCATCATCAGCTACCTGTGATACCGAACA |
| Genotyping | NeoAL2 | GGGGATGCGGTGGGCTCTATGGCTT |
| | SXR RC RV5 | TGAGAGTGCACAAGTTCAAGCT |
| | WTInt5 | AGTGATGGGAACCACTCCTG |
| | WTEx6RV | TGGTCCTCAATAGGCAGGTC |
| | mhSXRE4 | GTGAACGGACAGGGACTCAG |
| | mhSXRSARV | CTCTCCTGGCTCATCCTCAC |
| Percellome quantitative RT-PCR | Cyp3a11 FW | CAGCTTGGTGCTCCTCTACC |
| | Cyp3a11 RV | TCAAACAACCCCCATGTTTT |
| | Ces6 FW | GGAGCCTGAGTTCAGGACAGAC |
| | Ces6 RV | ACCCTCACTGTTGGGGTTC |
| | mouse SXR FW | AATCATGAAAGACAGGGTTC |
| | mouse SXR RV | AAGAGCACAGATCTTTCCG |
| | human SXR FW | ATCACCCGGAAGACACGAC |
| | human SXR RV | AAGAGCACAGATCTTTCCG |
| | mouse-human SXR FW | CCCATCAACGTAGAGGAGGA |

has the neomycin resistance gene with loxP sequence at both ends, removable with Cre recombinase (Saga *et al.*, 1999). A 7kb KpnI fragment containing intron 2 was used as a long arm and 1.3kb PstI-EcoRI fragment containing from exon 8 to intron 8 was used as a short arm for homologous recombination (Fig. 1). The resulting targeting vector was linearized with SacII and introduced by electroporation to TT2 ES cell line (Yagi *et al.*, 1993) and neomycin resistant clones were selected, PCR genotyped, and confirmed by the Southern blotting. For generation of chimeric mice, these ES clones were aggregated with ICR 8-cell embryos and transferred to pseudopregnant female recipients. The chimeric mice born were bred with ICR females. Germ line transmission of the targeted allele was confirmed by PCR. A mouse was crossed with a CAG-Cre transgenic mouse (Sakai and Miyazaki, 1997) to evict the neomycin resistance gene, and back crossed to C57BL/6 CrSlc (SLC, Inc., Shizuoka, Japan) at least 6 generations and used for the analysis.

### PCR Genotyping
### (See Table 1 for primer sequences)

Primers for identification of homologously recombined ES clones were NeoAL2 and SXR RC RV5. DNA purified from the tail of each mouse was used for PCR genotying. Primers for WT detection were WTInt5 and WTEx6RV amplifying a product of 755 bp. Primers for confirmation of removal of the neomycin resistance gene were mhSXRE4 and mhSXRSARV amplifying a product of 1,223 bp.

### Southern blot analysis

To confirm homologous recombination, DNA from ES cell cultures was purified and digested with BamHI and XhoI, then electrophoresed and analyzed by Southern hybridization (Saga *et al.*, 1997). Mouse SXR exon 9 region which remains after homologous recombination was used for the probe. The restriction fragments from the WT allele and targeted allele are 2,305 bp and 1,925 bp, respectively.

### Chemicals

RIF (molecular weight 822.95) and PCN (molecular weight 341.49) were purchased from Sigma-Aldrich (St. Louis, MO, USA). Corn oil was purchased from Wako Pure Chemical Industries (Osaka, Japan).

### Quantitative RT-PCR (Percellome PCR)
### (See Table 1 for primer sequences)

The method for Percellome quantitative RT-PCR was described previously (Kanno *et al.*, 2006). Briefly, tissue pieces stored in RNAlater (Ambion, Austin, TX, USA) were homogenized and lysed in RLT buffer (Qiagen GmbH., Germany) and 10 μl aliquots were used

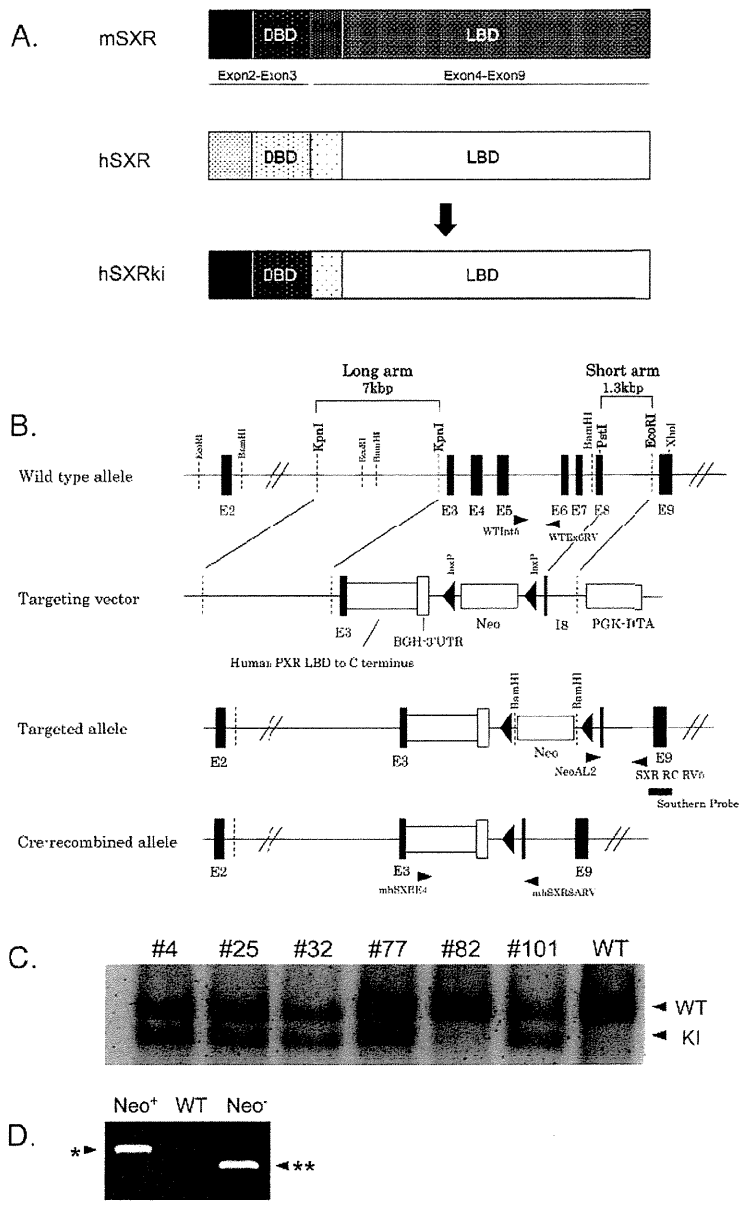


**Fig. 1.** Targeting strategy used to generate the hSXRki mouse. A) Diagram of hSXRki chimeric protein. Hinge region and ligand binding domain (LBD) of human SXR are knocked-in to mouse SXR, resulting in chimeric protein having murine N-ternial domain and DNA binding domain (DBD). B) Targeting strategy used to generate the hSXRki mouse. The chimeric mouse DBD and human LBD fragment, followed by the BGH 3' UTR were knocked-in to the mouse SXR gene. The genomic region spanning from exon 3 to exon 8 was substituted by the inserted fragment with the remainder of the gene remaining intact. C) Confirmation of homologous recombination by southern blot analysis. Six ES clones positive for recombination by PCR genotyping were further analyzed by southern blot (clones #4 ~ #101). Lower bands (1925 bp) indicate successful homologous recombination; upper bands (2305 bp) correspond to WT allele. Clones #4, #25, #32, #77 and #101 were confirmed as homologous recombinants; clones #4 and #25 were used for the generation of chimeric mice. D) Confirmation of Cre-mediated removal of the neomycin resistance gene. Mouse tail genome DNA was PCR amplified with the primer set, mhSXRE4 and mhSXRSARV. *: 2,858 bp (for the mice having the neomycin resistance gene), **: 1,223 bp (for the mice without the neomycin resistance gene).

for genomic DNA quantification with PicoGreen fluorescent dye (Invitrogen, Carlsbad, CA, USA). A prepared spike mRNA cocktail solution containing known quantity of five mRNAs of bacillus subtilis was added to the tissue lysate in proportion to the DNA quantity. Total RNA was purified from the lysate using the RNeasy kit (Qiagen). One microgram of total RNA was reverse-transcribed with SuperScript II (Invitrogen). Quantitative real time PCR was performed with an ABI PRISM 7900 HT sequence detection system (Applied Biosystems) using SYBR Green PCR Master Mix (Applied Biosystems), with initial denaturation at 95°C for 10 min followed by 40 cycles of 30 sec at 95°C and 30 sec at 60°C and 30 sec at 72°C, and Ct values were obtained. Primers for Cyp3a11 were Cyp3a11 FW and Cyp3a11 RV. Primers for Ces6 were Ces6 FW and Ces6 RV. Primers for mouse SXR selective quantification were mouse SXR FW and mouse SXR RV. Primers for hSXRki selective quantification were human SXR FW and human SXR RV. Primers for both mouse SXR and hSXRki quantification were mouse-human SXR FW and mouse-human SXR RV that amplify the DBD region of the chimera.

### *In Situ* Hybridization analysis

Digoxigein-labeled cRNA probe for Cyp3a11 was synthesized according to Suzuki *et al.* (2005) by RT-PCR using mouse liver cDNA as a template. The primers used were as follows: forward 5'-GATTGGTTTTGATGCCTGGT-3' and reverse 5'-CAAGAGCTCACATTTTTCATCA-3'. The amplified product was sequence confirmed and ligated with Block-iT T7-TOPO (Invitrogen) Linker, which contains the T7 promoter site. A secondary PCR was performed to generate the sense and antisense DNA templates. For antisense template, Block-iT T7 Primer and Cyp3a11 forward primer (or reverse primer for generation of sense DNA template), the same primer as for the first PCR amplification, were used. With these DNA templates, both sense and antisense digoxigenin-labeled riboprobes were synthesized using a DIG RNA labeling kit (Roche Diagnostics, Germany) according to the manufacturer's protocol.

ISH on paraffin sections was carried out according to Suzuki *et al.* with a modification; permeabilization condition 98°C for 15 min in HistoVT One (Nacalai tesque, Japan).

### Animals experiments

Male hSXRki and WT mice were maintained under a 12 hr light/12 hr dark cycle with water and chow (CRF-1, Oriental Yeast Co. Ltd., Tokyo, Japan) provided *ad libitum*. The animal studies were conducted in accordance with the Guidance for Animal Studies of the National Institute of Health Sciences under Institutional approval. The expression level of the hSXRki and WT SXR mRNA of ten organs (brain, thymus, heart, lung, liver, stomach, spleen, kidney, small intestine and testis) were analyzed on 15 weeks old male mice (n = 2) by the Percellome quantitative RT-PCR.

For the demonstration of selective gene induction by RIF and PCN in hSXRki and WT male mice on 13 weeks

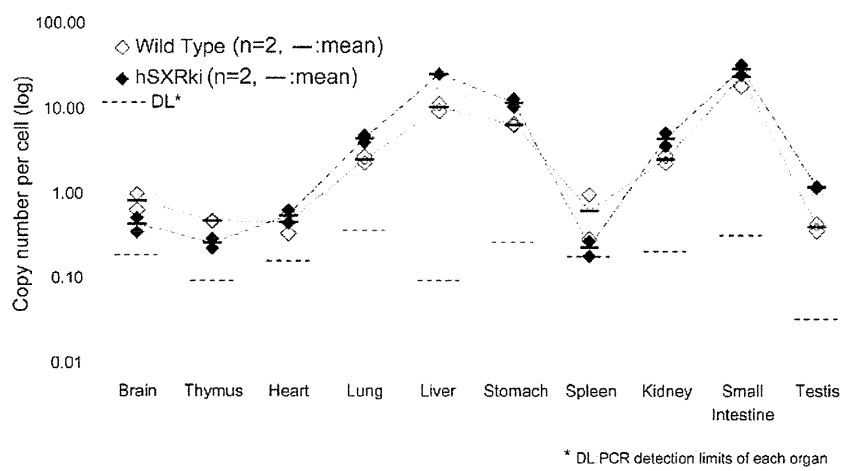


**Fig. 2.** Conservation of tissue expression patterns of hSXRki mRNA in the knock-in mouse. Percellome quantitative RT-PCR analysis was performed to measure the absolute expression levels of WT SXR mRNA and hSXRki mRNA in ten organs of WT and hSXRki mice. The expression levels of hSXRki mRNA among organs were comparable to WT.

old, three mice per group were singly dosed orally with vehicle (corn oil+0.1% DMSO), 10, 30, or 100 mg/kg of RIF, or 20, 70, or 200 mg/kg PCN (approximately equivalent in molar dose). Eight hours later, mice were sacrificed by exsanguination under ether anesthesia and the liver and the small intestine mucosa were sampled. Liver samples in small pieces were stored in RNA later (Applied Biosystems, Foster City, CA, USA) for further analysis. The small intestine under ice-cooled condition was longitudinally opened, gently rinsed with RNase-free saline and the epithelium was scraped with a glass slide and immersed in RNAlater. For *in situ* hybridization (ISH) of Cyp3a11 in the liver, 15 weeks old male hSXRki and WT mice were dosed orally with vehicle (corn oil), RIF (10 mg/kg), or PCN (40 mg/kg) daily for 3 days and liver sampled 24 hr later. All mice were sacrificed by exsanguination under ether anesthesia.

### Statistical analysis

All values are expressed as the means ± S.D. and group differences analyzed by unpaired Student's *t* test or one-way ANOVA followed by Dunnett's post hoc comparison. Level of significance was set at $p < 0.05$.

## RESULTS

### Generation of hSXRki knock-In mice

Among 144 neomycin resistant TT2 ES clones, six PCR positive clones were further submitted to Southern blotting for the confirmation of homologous recombination. As shown in Fig. 1C, five clones were confirmed, and two (#4 and #25) were used to generate chimeric mice. The resulting mice were backcrossed to ICR strain to confirm germline transmission. One clone (#4) was crossed to a mouse constitutively expressing Cre recombinase to remove the neomycin resistance gene (Fig. 1D) and backcrossed to C57BL/6 CrSlc for at least 6 generations before further analysis.

### Tissue distribution of hSXRki mRNA

Ten tissues, i.e., brain, thymus, heart, lung, liver, stomach, spleen, kidney, small intestine and testis from both hSXRki and WT mice were measured for hSXRki or WT SXR mRNA expression by the Percellome quantitative RT-PCR. As shown in Fig. 2, the levels of hSXRki mRNA are comparable to that of SXR in WT mouse and expressed in all tissues analyzed.

### Humanized responses in hSXRki mouse

Humanized response of hSXRki was demonstrated by administration of the mouse-specific ligand PCN and the

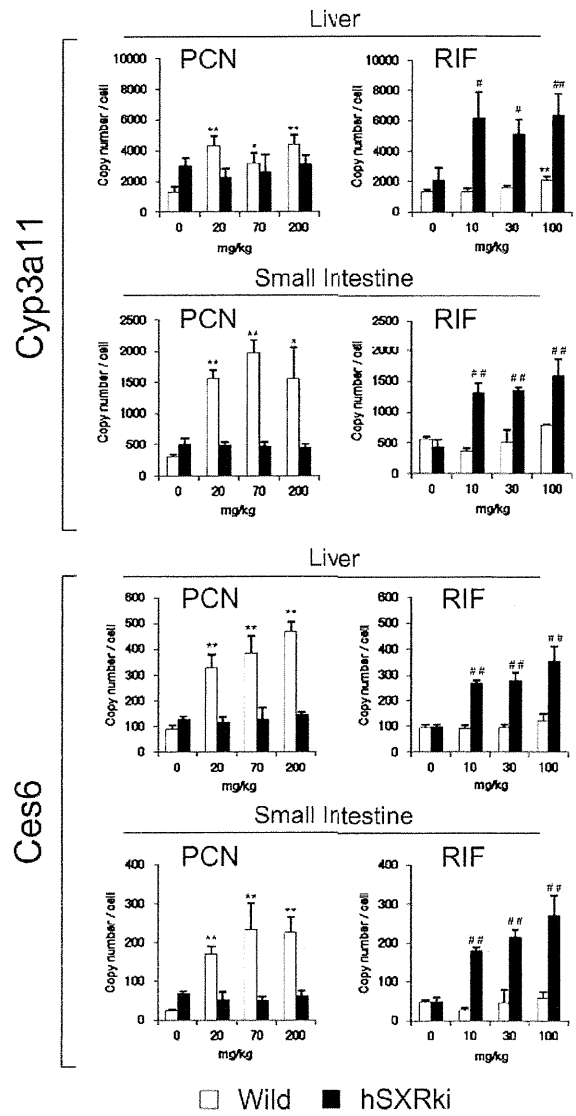


**Fig. 3.** Humanized response of hSXRki mice to RIF and PCN; Percellome quantitative RT-PCR. WT mice and hSXRki mice (n = 3 each) were singly dosed orally with vehicle (corn oil+0.1% DMSO), 20, 70, or 200 mg/kg PCN, or 10, 30, or 100 mg/kg of RIF (approximately equivalent in molar dose each other). Percellome quantitative RT-PCR data of Cyp3a11 and Ces6, both known as SXR target genes, in liver and small intestinal mucosa showed humanized responses in hSXRki. Bars = S.D., *; $p < 0.05$, **; $p < 0.01$ compared with vehicle group of WT, #; $p < 0.05$, ##; $p < 0.01$ compared with vehicle group of hSXRki. Analyzed by one-way ANOVA followed by Dunnett's post hoc comparison. Level of significance was set at $p < 0.05$.

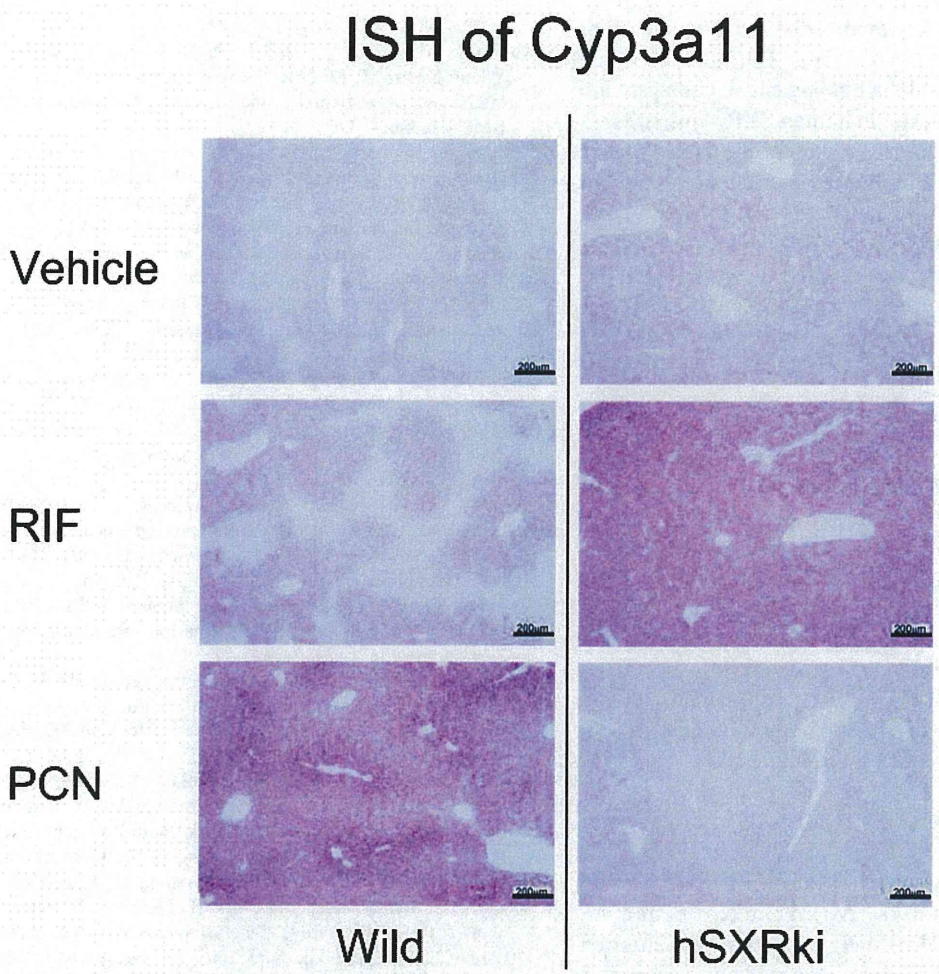


**Fig. 4.** Humanized response of hSXRki mice to RIF and PCN; *In situ* hybridization for Cyp3a11 mRNA in liver. A DIG-labeled cRNA probe for Cyp3a11 was hybridized and developed for purplish blue chromogenic reaction. Histologically, Cyp3a11 induction was localized around the central veins in both mice with species-specific ligands, respectively.

human-specific ligand RIF to the mice. Induction of the well-known SXR-regulated genes, Cyp3a11 and Ces6 was monitored by Percellome quantitative RT-PCR. As shown in Fig. 3, in the liver and small intestinal mucosa, RIF, but not PCN, induced Cyp3a11 and Ces6 in hSXRki mice (closed column), whereas PCN exclusively induced these genes in WT mice (open column). ISH of Cyp3a11 of the liver also showed humanized responses in hSXRki mice (Fig. 4).

## DISCUSSION

We generated a new humanized mouse model in which the ligand binding domain (LBD) of human SXR was homologously knocked-into the murine SXR gene so that systemic response induced by human-selective SXR ligands can be monitored in mice. Firstly, we showed that mRNA from this chimeric gene was expressed at appropriate levels in the same tissues as the endogenous mouse SXR gene in WT mice. Then the humanized response of the mouse was confirmed by monitoring its response to the human-selective activator RIF, and the lack of response to the rodent-selective activator PCN.